AJR FOCUS ON:

PET Molecular Imaging–Directed Biopsy: A Review

Baowei Fei[1,2,3]
David M. Schuster[1,3]

OBJECTIVE. The purpose of this review is to summarize the applications of PET molecular imaging–directed biopsy of a variety of organs in the management of various diseases with a focus on cancers.

CONCLUSION. PET can yield metabolic information at the cellular and molecular levels, and PET-directed biopsy is playing an increasing role in the diagnosis and staging of diseases.

Keywords: biopsy, molecular imaging, PET

DOI:10.2214/AJR.17.18047

Received February 3, 2017; accepted without revision February 27, 2017.

Supported in part by NIH grants CA176684, R01CA156775, and CA204254 and by developmental funds from the Winship Cancer Institute of Emory University under award P30CA138292.

The authors have participated in sponsored research involving ^{18}F-fluciclovine among other radiotracers. Emory University is eligible to receive royalties for ^{18}F-fluciclovine.

[1]Department of Radiology and Imaging Sciences, Emory University School of Medicine, 1841 Clifton Rd NE, Atlanta, GA 30329. Address correspondence to B. Fei (bfei@emory.edu).

[2]Department of Biomedical Engineering, Emory University and Georgia Institute of Technology, Atlanta, GA.

[3]Winship Cancer Institute of Emory University, Atlanta, GA.

This article is available for credit.

AJR 2017; 209:255–269

0361–803X/17/2092–255

PET molecular imaging has been widely used in oncology and other applications. This review focuses on PET image-directed biopsy for the diagnosis and staging of various diseases. A PubMed search was performed in January 2017. The search strategy consisted of the terms "PET," "positron emission tomography," "guided OR guidance," "biopsy," and combinations of these terms in titles and abstracts. The literature from the search results was recorded and further selected after the abstracts were read. This review covers PET-guided biopsy involving nearly all organs and tissues in the body.

Brain

For more than 2 decades ^{18}F-FDG PET has been used in the selection of brain lesions for biopsy. In 1991, Hanson et al. [1] used FDG PET to determine the site most likely to yield a diagnostic biopsy result. That study showed a complementary role of FDG PET and CT or MRI in the care of selected patients for defining the intracranial site most likely to yield a positive biopsy result. In 1992, Levivier et al. [2] defined a technique that allowed target definition for stereotactic brain biopsy through the use of coordinates calculated on stereotactic PET images. Because of the complementary roles of PET and CT, their integration in multimodality planning optimized target selection for stereotactic brain biopsy [3]. Levivier et al. [4] also studied whether routine integration of FDG PET in the planning of stereotactic brain biopsy increases the diagnostic yield of the technique. That study showed that FDG PET contributed to the treatment of brain tumor patients who needed stereotactic biopsy. In 1995, Pirotte and colleagues [5, 6] reported on multiple studies of PET-guided stereotactic brain biopsy. They described a technique allowing routine integration of PET scan data in the planning of stereotactic brain biopsy for patients who had undergone combined FDG PET and CT-guided stereotactic biopsy. They integrated PET images into the planning for stereotactic biopsy procedures to direct the biopsy needle trajectory to hypermetabolic foci of intrinsic infiltrative brainstem lesions.

By integrating FDG PET in the planning of stereotactic brain biopsy, Goldman et al. [7] investigated whether the glucose metabolism of gliomas is related to anaplasia and whether FDG PET depicts metabolic heterogeneity that parallels the histologic heterogeneity of gliomas. This early study showed that FDG uptake in gliomas is anatomically heterogeneous and regionally related to the presence of anaplasia. In 2013, Koethe et al. [8] reported that PET-guided biopsy with needle navigation facilitates the diagnosis of angiosarcoma in neurofibromatosis. In the latest development, PET/CT-based metabolic imaging has been integrated with standard MRI-guided stereotactic biopsy. Zhao et al. [9] investigated the clinical value of intraoperative MRI coregistration combined with PET/CT for stereotactic brain biopsy. Compared with intraoperative MRI only, the combined treatment improves the diagnostic success rate without increasing complications [9].

Studies have been conducted to compare PET performed with ^{11}C-methionine (MET) and FDG for guidance of brain biopsy. Pirotte and colleagues [10, 11] compared the contributions of MET and FDG for PET-guided stereotactic biopsy of brain gliomas. PET images were analyzed to determine which radiotracer offered the best information for target definition. The study results showed that distributions of the highest MET and FDG uptake are similar in brain gliomas. Because MET provides a more sensitive signal, it is the molecule of choice for single-radiotracer PET-guided neurosurgical procedures for glioma [10, 11]. In another study, Pirotte et al. [12] assessed the benefit of the technique in terms of target selection and diagnostic yield. Patients with newly diagnosed intrinsic infiltrative brainstem lesions underwent PET-guided stereotactic biopsy. A single biopsy target was selected in the area of highest PET tracer uptake. Use of PET guidance improved the target selection and allowed tumor diagnosis in all trajectories. The PET-guided trajectories had higher diagnostic yield than those guided by MRI alone and allowed reduction of sampling to a single trajectory.

PET guidance improves the diagnostic yield of stereotactic biopsy sampling, allows the clinician to reduce the number of sampling procedures, and leads to a reassessment of the utility of and indications for stereotactic biopsy in children with intrinsic infiltrative brainstem lesions. Kawai et al. [13] described a patient with germinoma in the basal ganglia that had nonspecific clinical and radiologic findings and found MET PET useful for locating the optimal biopsy target and monitoring treatment efficacy. In a study by Goldman et al. [14], local histologic characteristics were used to confirm the regional uptake of FDG and MET in patients with high-grade glioma diagnosed during PET-guided stereotactic biopsy. Both MET PET and FDG PET were useful for in vivo evaluation of the metabolic heterogeneity of human gliomas. These results underline the complementary role of FDG and MET for the study of brain tumors and favor the use of these agents for stereotactic PET guidance of diagnostic procedures.

Other radiotracers have been used for the guidance of brain biopsies. Go et al. [15] used spectroscopic MRI and L-1-^{11}C-tyrosine PET to localize cerebral gliomas for biopsy. Hara et al. [16] used ^{18}F-choline and ^{11}C-choline for PET-guided stereotactic biopsy sampling of gliomas. The PET scans of gliomas in which ^{18}F- and ^{11}C-choline were used to guide the approach to the most malignant areas for stereotactic sampling. Amino acid ^{18}F-fluoroethyl-tyrosine PET (FET PET) has been used to identify metabolically active tumor tissue and to differentiate it from therapy-associated changes. A study by Misch et al. [17] showed that the indications for FET PET were visualization of metabolically active malignant tissue within anatomically defined lesions or previously treated tumors and assessment of their extent (Fig. 1). FET PET was helpful for target selection and was integrated into surgical guidance. FET PET image–guided surgical targeting yielded histologic diagnoses with appropriate specificity and high sensitivity in the care of pediatric brain tumor patients.

Lopez et al. [18] correlated the histopathologic criteria of biopsy sites with PET uptake values. They analyzed the diagnostic value of PET by comparing the FET PET findings in patients with newly diagnosed brain lesions with the histologic findings obtained from stereotactic serial biopsy. FET PET allowed differentiation of high-grade glioma from low-grade glioma. In a 2016 study, Kondo et al. [19] found that anti-^{18}F-fluciclovine PET/CT can delineate glioma spread that is undetectable at contrast-enhanced T1-weighted MRI and can be used to guide glioma biopsy.

Pafundi et al. [20] compared ^{18}F-dihydroxyphenylalanine (DOPA) PET with conventional MRI for neurosurgical biopsy targeting, resection planning, and radiotherapeutic target volume delineation. The study showed that regions of higher-grade and higher-density disease were accurately identified with DOPA standardized uptake values in patients with astrocytomas and that DOPA PET was useful for guiding stereotactic biopsy selection. Price et al. [21] compared regional variations in the uptake of ^{18}F-fluorothymidine (FLT) PET images with measures of cellular proliferation from biopsy specimens obtained at image-guided brain biopsies. Patients with a supratentorial glioma that required image-guided brain biopsy underwent preoperative imaging with dynamic PET after administration of FLT. Maps of the FLT irreversible uptake rate and the standardized uptake value were calculated. These maps were coregistered to a gadolinium-enhanced T1-weighted spoiled gradient-echo MR image that was used for biopsy guidance. The study showed that FLT PET was a useful marker of cellular proliferation that correlates with regional variation in cellular proliferation.

Because MRI alone has limitations in target selection for biopsy or resection in patients with newly diagnosed or pretreated brain tumors, the combination of PET and MRI or in vivo MR spectroscopy (MRS) allows noninvasive imaging of cellular metabolism relevant to proliferation and can depict regions of more highly active tumor. Masada et al. [22] used coregistered PET and MR images to determine the biopsy target and performed brain biopsy guided by a stereotactically inserted tube. The coregistered PET and MR images depicted the most active region of the brain tumor.

Guo et al. [23] assessed the value and feasibility of PET/MRI fusion technology for delineating tumor boundaries and positioning biopsy targets of gliomas to facilitate the diagnosis and treatment of gliomas. They used MRI, FDG PET, and fluoroethylcholine (FECH) PET in the study. With regard to patients who underwent both biopsy and tumor resection, the pathologic diagnosis of the specimen obtained from the PET-guided biopsy was consistent with that of subsequently resected tissue. PET-MRI fusion accurately delineated the tumor boundary and sensitively targeted the region of high proliferation or metabolism.

Grech-Sollars et al. [24] integrated presurgical PET and MRS with intraoperative neuronavigation to guide surgical biopsy and tumor sampling of brain gliomas to improve intraoperative tumor-tissue characterization and imaging biomarker validation. They developed an intraoperative neuronavigation tool as part of the study with the intention of sampling high-choline tumor components identified with multivoxel MRS and ^{18}F-methylcholine PET/CT. Spatially coregistered PET and MRS data were integrated into structural datasets and loaded into an intraoperative neuronavigation system. Regions of high and low uptake of choline and metabolites were represented as color-coded, hollow spheres for targeted stereotactic biopsy and tumor sampling. These PET and MRI data were combined for the surgeon in neuronavigation systems. This multimodality imaging method enabled neurosurgeons to sample tumor regions based on physiologic and molecular imaging markers.

Bone

FDG PET and ^{99m}Tc–methylene diphosphonate bone scintigraphy are useful imag-

ing modalities for detecting skeletal metastases. PET is believed to be more specific than bone scintigraphy for detecting malignancy [25]. Pezeshk et al. [25] investigated the value of PET compared with bone scintigraphy for directing biopsies in patients with suspected metastatic bone lesions. The results of their study support the use of PET to effectively direct bone biopsies to confirm the presence of metastatic neoplasms. The results also suggest that PET may incrementally improve the diagnostic yield over that of bone scintigraphy.

Other studies [26–29] have shown FDG PET/CT useful for bone and soft-tissue biopsy. Werner et al. [26] reported a case of FDG PET/CT–guided biopsy of bone metastases. Purandare et al. [28] studied whether the metabolic information provided by a previous PET/CT scan can add valuable information and be of incremental benefit during the performance of image-guided biopsies. The biopsy sites included bone, lung, lymph nodes, and soft-tissue masses. PET/CT data were coregistered with intraprocedural CT images and were used to guide needle placement in the viable portion of a lesion, increasing the chances of achieving a definitive diagnosis. This approach offered a substantial incremental benefit in the performance of image-guided biopsies.

Maybody et al. [29] reported results on a patient with a clinical diagnosis of tumor-induced osteomalacia in whom the culprit tumor was localized with ^{68}Ga-tetraazacyclododecanetetraacetic acid–Phe1-Tyr3-octreotide PET/CT and MRI, and the biopsy was performed under PET/CT guidance. Guo et al. [30] evaluated the safety and efficacy of FDG PET/CT for guiding biopsy of bone metastases in patients with advanced lung cancer. PET/CT-guided percutaneous core biopsies were performed for patients with suspected lung cancer and FDG-avid bone lesions after whole-body FDG PET/CT. PET/CT-guided percutaneous biopsy of FDG-avid bone metastases is an effective and safe method that has a high diagnostic success rate in the evaluation of hypermetabolic bone lesions in patients with suspected advanced lung cancer.

Lymph Nodes

FDG PET plays an important role in lymph node biopsies. Kim et al. [31] designed a study to determine whether preoperative FDG PET integrated with CT can be used as a guide for axillary node dissection and sentinel lymph node biopsy (SLNB) in breast cancer patients, reducing the number of unnecessary SLNBs and thus enhancing the identification rates of sentinel nodes and the accuracy of SLNB. Purandare et al. [28] studied whether the metabolic information obtained in a previous PET/CT scan can add valuable information and an incremental benefit during image-guided biopsies. The patients' FDG PET/CT findings were available before biopsy. Biopsies were performed with standard techniques only after the needle tip was confirmed to be in the portion of the lesion corresponding to the hypermetabolic area on PET images. This was achieved by visual coregistration and by use of software registration algorithms that registered the intraprocedural CT images with the preselected PET/CT data. The study showed that PET/CT data coregistered with intraprocedural CT images could guide needle placement in the viable portion of the lesion, increasing the chances of achieving a definitive diagnosis. This approach added significant incremental benefit to performing image-guided biopsies. Challa et al. [32] studied the role of FDG PET/CT in the evaluation of axillary lymph node involvement and compared the results with those of SLNB. Their study showed that FDG PET/CT has low sensitivity but high specificity in the evaluation of axillary lymph node involvement in patients with breast cancer.

PET has been used in various lymph node biopsies. Siepel et al. [33] reported on a study of targeted mediastinoscopic lymph node biopsy performed with 3D FDG PET/CT videos. The feasibility and potential value of 3D FDG PET/CT videos were investigated to improve the accuracy of targeted lymph node biopsy during mediastinoscopy. PET/CT images were rendered in 3D volumes with multiplanar reconstructions and maximum intensity projections and were reviewed in 3D fly-through and fly-around videos. The results showed that use of PET/CT videos may reduce the frequency of false-negative mediastinoscopic findings and improve the staging of lung cancer. The study showed that 3D FDG PET/CT may be a promising tool for further implementation of image-guided surgery. Györke et al. [34] described a case of lymphoma in which an occult lesion localization method was used for radioguided biopsy of a chemoresistant lymph node detected with interim FDG PET/CT. Biopsy of the metabolically active, nonpalpable lymph node was performed with ultrasound guidance (Fig. 2). Juweid et al. [35] reported on the potential use of the interim FDG standardized uptake value for determining the need for a residual mass biopsy after dose-dense immunochemotherapy for advanced diffuse large B-cell lymphoma.

Breast

The use of PET in the care of patients with breast cancer has been limited by the lower levels of FDG uptake in some breast malignancies than in other cancers, the small size of many breast cancers, and the need for biopsy under PET guidance. High-resolution breast PET, or positron emission mammography (PEM), with biopsy guidance software is a new direction. Kalinyak et al. [36] reported the results of a prospective multicenter study designed to test the efficacy and safety of PEM biopsy guidance software for women with FDG-avid breast lesions worrisome for malignancy. The intervention chosen was vacuum-assisted core biopsy. The study showed that high-resolution PEM-guided breast biopsy is safe and effective for the sampling of PET-visualized breast lesions. Raylman et al. [37] described the design of a PEM-PET breast imaging and biopsy system. The PEM-PET scanner consists of two sets of rotating planar detector heads. PET images are acquired to detect suspicious focal uptake of the radiotracer and guide biopsy of the area. The PEM-PET system may be a new tool for the detection and biopsy of breast cancer in the future.

Chest

Once lung cancer is discovered, accurate staging at baseline is imperative to maximize patient benefit and cost-effective use of health care resources. Although CT remains a powerful tool for the staging of lung cancer, advances in other imaging modalities, specifically PET/CT and MRI, can improve the baseline staging over that of CT alone and can allow more rapid and accurate assessment of the treatment response [38]. FDG PET has been considered a "metabolic biopsy" [39] tool in the evaluation of nonlung lesions with indeterminate biopsy results. Niida et al. [40] reported a case in which pulmonary intravascular lymphoma was diagnosed with FDG PET–guided transbronchial lung biopsy. Purandare et al. [28] found that lung biopsies were performed only after the needle tip was confirmed to be in the portion of the lesion corresponding to the hypermetabolic area seen on PET images. This

was achieved by visual coregistration and by the use of software registration algorithms that registered the intraprocedural CT images with the preselected PET/CT data. Their study showed that PET/CT data coregistered with intraprocedural CT images could guide needle placement in the viable portion of the lesion and thus increase the chances of achieving a definitive diagnosis. Collins et al. [41] reported that CT-guided, fine-needle aspiration (FNA) biopsies performed with FDG PET scans of pulmonary lesions contributed substantially to the management and treatment of pulmonary disease.

İntepe et al. [42] compared the results of transthoracic needle biopsies performed with and without FDG PET/CT. Their study showed that using FDG PET/CT to guide transthoracic biopsy increases the rate of accurate diagnosis (Fig. 3). Lin [43] reported a case in which FDG PET/CT was used for biopsy guidance in a patient with Erdheim-Chester disease. The PET/CT was important in identifying an area for biopsy and for visualizing bone involvement. Yokoyama et al. [44] compared the results of CT-guided, percutaneous biopsy with and without registration of previous PET/CT images in the diagnosis of mediastinal tumors. The study showed that PET/CT is not typically needed because CT-guided percutaneous biopsy can yield a precise diagnosis of most mediastinal tumors. It also showed that PET/CT-guided biopsy had no special diagnostic advantages.

PET has also been used as a noninvasive imaging modality for the staging of esophageal cancer [45]. Mizugaki et al. [46] evaluated the combination of transbronchial biopsy and endobronchial sonography with a guide sheath (EBUS-GS) and FDG PET for the diagnosis of small peripheral pulmonary lesions. The combination of transbronchial biopsy with EBUS-GS and FDG PET is useful for the diagnosis of these small lesions. Combined FDG PET/CT– and CT-guided biopsy has also been used for diagnosing recurrence of esophageal cancer [47].

Head and Neck

In the assessment of locally recurrent and metastatic head and neck neoplasia, FNA biopsy and FDG PET are highly sensitive for identifying tumors in patients with clinically suspected recurrence and locally metastatic disease [48]. FNA biopsy can yield confirmatory evidence of disease in a clinically suspicious abnormality with nonspecific FDG PET results. Kovács et al. [49] reported that PET in combination with SLNB reduces the rate of elective neck dissections in the treatment of oral and oropharyngeal cancer. Compared with CT, PET in combination with lymphoscintigraphy-guided SLNB considerably reduces the number of extensive neck dissections in patients with oral and oropharyngeal squamous cell carcinoma. Reinbacher et al. [50] described a method of 3D image–guided biopsy of orbital tumors using a combined technique of hardware fusion between FDG PET, MRI, and CT. The method allows minimally invasive biopsy even of deep intraconal lesions and allows the surgeon to spare critical anatomic structures (Fig. 4).

Abdomen and Pelvis

PET has a major role in the diagnosis and staging of abdominal and pelvic diseases, especially liver and prostate cancer. Tatli et al. [51] developed a technique for guiding percutaneous biopsies of abdominal masses using a PET/CT scanner. After completion of the PET/CT scan, with the patient remaining on the table, a one-table-position PET/CT scan was obtained with a radiopaque grid in place, and the biopsy procedure was planned. A biopsy needle was then placed into the mass by use of a one-table-position CT scan registered to the planning PET scan. Masses were sampled after confirmation of accurate positioning of the needle tip with a final, one-table-position PET/CT scan. The study results suggested that abdominal masses can be successfully biopsied with a PET/CT scanner.

Tatli et al. [52] also studied the feasibility of performing combined PET/CT-guided biopsy of abdominal masses using previously acquired PET/CT images registered with intraprocedural CT images. PET/CT-guided abdominal biopsy using previous PET/CT images registered with intraprocedural CT scans was helpful for biopsy sampling of FDG-avid masses not seen sufficiently with unenhanced CT.

Aparici and Win [53] reported the case of a patient for whom FDG PET/CT was used to perform biopsy of a mesenteric mass. Real-time intraprocedural PET-guided biopsy of a new mesenteric mass revealed Bcl-2–positive, poorly defined lymphoid follicles compatible with follicular lymphoma (Fig. 5). PET/CT-guided biopsy allowed early histologic diagnosis and staging before morphologic changes were evident by allowing sampling of the metabolically active part of the lesion.

Liver

Shao et al. [54] investigated the accuracy of PET/CT- and ultrasound-guided biopsy for the diagnosis of liver carcinomas. Before surgery, patients underwent PET/CT assessment, an ultrasound examination, and ultrasound-guided biopsy of liver tissue. The combined use of PET/CT, ultrasound assessment, and ultrasound-guided biopsy can improve the diagnosis of liver cancer. FNA biopsy is a well-described diagnostic method for evaluation of hepatic lesions. The FDG PET scan, combined with FNA biopsy, can provide reliable diagnostic information and assist in the guidance of oncologic patient care [55]. Yu and Sheng [56] reported a case in which liver tuberculosis presented as an uncommon cause of pyrexia of unknown origin and in which PET/CT helped to identify the correct site for biopsy. Ewertsen et al. [57] reported that the use of fusion-guided sonography facilitated conclusive diagnosis regarding lesions in the liver seen at CT, MRI, or PET/CT. The study showed an increase in characterization of liver lesions with fusion-guided ultrasound compared with conventional B-mode ultrasound. Imperiale et al. [58] reported the results of simultaneous ^{18}F-fluorodihydroxyphenylalanine PET/CT-guided biopsy in a patient with hepatic metastatic evolution of a well-differentiated ileal neuroendocrine tumor. The study showed that PET/CT-guided biopsy is useful for confirming the metabolic findings when conventional imaging does not show morphologic abnormalities (Fig. 6).

Prostate

PET can depict metabolic and functional information about prostate cancer. Various PET agents were developed or are under development for prostate cancer detection. PET with new molecular imaging radiotracers, such as choline, prostate-specific membrane antigen, and fluciclovine, has had promising results in the detection and localization of prostate cancer in humans [59, 60]. For patients with previous negative biopsy results but elevated prostate-specific antigen (PSA) levels, PET-guided biopsy can have an important role in the management of prostate cancer.

Fei and colleagues [61–64] developed an approach to PET molecular image–directed 3D ultrasound–guided biopsy. The components of the targeted biopsy system are passive mechanical components for guiding, tracking, and stabilizing the position of a commercially available transrectal ultrasound probe; soft-

ware for acquiring and reconstructing a series of real-time 2D transrectal ultrasound image slices into a 3D image volume of the prostate; and software that segments the prostate gland in the 3D transrectal ultrasound image volume and then displays a 3D model to guide a biopsy needle to the suspicious target lesions in three dimensions. The system allows real-time tracking and recording of the 3D position of the biopsy sites as a physician manipulates the ultrasound transducer. An offline workstation system is used to register and fuse PET/CT and ultrasound images.

The clinical work flow for PET/CT-directed, 3D ultrasound–guided biopsy of the prostate includes the following steps. First, before undergoing the targeted biopsy, the patient undergoes PET/CT as part of his evaluation. The anatomic CT images are registered with the PET images for improved localization of the prostate and suspicious lesions. Second, the patient undergoes 3D ultrasound (prebiopsy image) before the actual biopsy appointment. This planning scan may be obtained at any time before the biopsy and even on the same day as the PET/CT examination. Third, the PET/CT and prebiopsy ultrasound images are registered offline before biopsy. Fourth, another 3D ultrasound image volume is acquired immediately before the biopsy planning. These intrabiopsy ultrasound images are registered with the prebiopsy ultrasound image volume. As the prebiopsy ultrasound image volume was registered with the PET/CT volumes, in turn the PET/CT image is registered with the intrabiopsy ultrasound image volume for tumor targeting. Three-dimensional visualization tools are then used to guide the biopsy needle to a suspicious lesion. Fifth, the position of the needle tip is recorded on real-time ultrasound images during the biopsy procedure. The location information on biopsy cores is saved and can be restored in a rebiopsy procedure if necessary. This allows the physician to rebiopsy the same area and monitor the potential progression of or treatment effects on a lesion. The location information on the biopsy cores can also be used to guide an additional biopsy to different locations if the original biopsy results were negative.

PET with ^{11}C-choline and ^{18}F-choline has been used to guide prostate biopsies. Freesmeyer et al. [65] reported a case in which atypical cancer recurrence in the right distal lower leg was suspected at FECH PET/CT of a patient with a history of prostate cancer and an increased PSA level. A PET-ultrasound fusion technique was used to localize the tumor and perform a biopsy, which led to a final diagnosis of peripheral schwannoma. Garcia-Bennett et al. [66] reported a case of ^{18}F-choline PET/CT detection of a needle track recurrence after transrectal prostate biopsy.

Kwee and DeGrado [67] reported a case of prostate biopsy guided by ^{18}F-fluorocholine PET in a patient with persistently elevated PSA levels. In a study by Igerc et al. [68], patients with persistently elevated PSA levels and negative prostate biopsy results were evaluated with ^{18}F-choline PET/CT to delineate prostate cancer and guide repeat prostate biopsy. After PET/CT, all patients underwent a repeat prostate biopsy, and in the cases in which focal or multifocal uptake was found, the biopsy was guided by the results of the examination. The results of the study show that ^{18}F-choline cannot be generally recommended for localizing primary prostate cancers.

Takei et al. [69], however, reported a case of multimodality multiparametric ^{11}C-choline PET/MRI for biopsy targeting in previously biopsy-negative primary prostate cancer. For targeting rebiopsy, the patient underwent ^{11}C-choline PET/CT and subsequent PET/MRI. Both the high uptake at PET and the abnormal findings at MRI were strong evidence of prostate cancer at the ventral periphery of the right apex (Fig. 7). This location is sometimes not covered by routine sextant biopsy, and the subsequent targeted rebiopsy was positive for prostate cancer. This case indicates the potential role of PET/MRI for identifying primary prostate cancer because of its high soft-tissue contrast and the possibility of a multimodality approach.

PET with other tracers has also been used to direct prostate biopsy. Jadvar et al. [70] reported the case of a patient with prostate cancer who had an elevated PSA level and had undergone a previous standard transrectal ultrasound biopsy with negative results and then underwent clinical 3-T multiparametric MRI and PET/CT with the cellular proliferation radiotracer ^{18}F-labeled 2′-fluoro-5-methyl-1-β-D-arabinofuranosyluracil (FMAU). PET/CT and multiparametric MR images were fused with transrectal ultrasound images for hybrid image-based targeting of the biopsy needle. FMAU PET/CT was helpful in localizing the nonstandard biopsy sites that histopathologic analysis revealed to be tumor deposits.

Muscles

The development of FDG PET/CT has made it possible to identify many unsuspected lesions, such as isolated intramuscular metastases, because it depicts abnormal metabolic activity at an early stage, even without clinical symptoms or morphologic changes [71]. PET/CT has been used to localize the primary lesion, identify a site to biopsy, and evaluate metastatic lesions that require follow-up biopsy [72] (Fig. 8). Mallarajapatna et al. [71] described a technique in which fused PET/CT was used to guide the percutaneous biopsy needle for sampling of isolated intramuscular metastatic lesions in a patient with intramuscular metastases identified only with PET/CT, not CT or ultrasound, and were clinically occult. Not all malignant tumors have hypermetabolic activity at PET, and many benign lesions and physiologic processes cause increased FDG uptake. Knowledge of these issues is important in reviewing PET/CT images and directing subsequent musculoskeletal biopsies [72].

Sarcoma

For soft-tissue masses, FDG PET has been found to be useful in identifying malignancy and variations in grade. MRI has been the most useful tool in the anatomic definition of soft-tissue sarcoma, although there remains the problem of defining the lesions as benign or malignant. Hain et al. [73] assessed the use of FDG PET with or without coregistered MR images to indicate the most appropriate biopsy site. All patients underwent MRI and FDG PET, and the two images were coregistered. A biopsy site that was the most likely to be malignant was defined on the PET scan. Patients underwent an initial biopsy and then complete resection of the mass. The histologic results from the mass were compared with those from the biopsy specimen obtained from the site suggested by the PET findings. The study showed that FDG PET can be used to appropriately direct biopsy of soft-tissue sarcoma and potentially lead to CT- or MRI-directed outpatient biopsy before definitive treatment.

Specimen

With PET-guided biopsy, the in vivo imaging findings can be directly correlated with the histologic results of biopsy specimens. Fanchon and colleagues [74, 75] developed a procedure for accurate determination of PET radiotracer concentration with high spatial accuracy in situ by performing quantitative autoradiography of biopsy specimens extracted under PET/CT guidance (Fig. 9). The biopsy sites were determined with PET/CT

images obtained in the operating room. Additional CT scans were acquired with the needles in place to confirm correct needle placement. Autoradiography was used to quantify the activities of biopsy specimens obtained under FDG PET guidance. The PET-guided approach and quantification method helped verify biopsy adequacy through a comparison of specimen activity and that expected from the PET image.

Conclusion

PET-directed biopsy has an increasing role in the diagnosis and staging of various diseases. Molecular image–guided biopsy approaches have great potential to increase the detection rate and improve diagnostic accuracy and therefore can have immediate impact on treatment decisions and patient care.

References

1. Hanson MW, Glantz MJ, Hoffman JM, et al. FDG-PET in the selection of brain lesions for biopsy. *J Comput Assist Tomogr* 1991; 15:796–801
2. Levivier M, Goldman S, Bidaut LM, et al. Positron emission tomography-guided stereotactic brain biopsy. *Neurosurgery* 1992; 31:792–797; discussion, 797
3. Levivier M, Goldman S, Pirotte B, Brotchi J. First year experience using the Fischer ZD–neurosurgical localizing unit with particular reference to the development of PET-guided stereotactic biopsy. *Acta Neurol Belg* 1993; 93:5–22
4. Levivier M, Goldman S, Pirotte B, et al. Diagnostic yield of stereotactic brain biopsy guided by positron emission tomography with [^{18}F]fluorodeoxyglucose. *J Neurosurg* 1995; 82:445–452
5. Pirotte B, Goldman S, Brucher JM, et al. PET in stereotactic conditions increases the diagnostic yield of brain biopsy. *Stereotact Funct Neurosurg* 1994; 63:144–149
6. Pirotte B, Goldman S, Bidaut LM, et al. Use of positron emission tomography (PET) in stereotactic conditions for brain biopsy. *Acta Neurochir (Wien)* 1995; 134:79–82
7. Goldman S, Levivier M, Pirotte B, et al. Regional glucose metabolism and histopathology of gliomas: a study based on positron emission tomography-guided stereotactic biopsy. *Cancer* 1996; 78:1098–1106
8. Koethe Y, Widemann BC, Hajjar F, Wood BJ, Venkatesan AM. PET-guided biopsy with needle navigation facilitates diagnosis of angiosarcoma in neurofibromatosis type 1. *Pediatr Blood Cancer* 2013; 60:E166–E169
9. Zhao JW, Chen ZJ, Wang ZG, et al. Stereotactic brain biopsy guided by iMRI co-registration combined with PET/CT. *Zhonghua Yi Xue Za Zhi* 2016; 96:685–688
10. Pirotte B, Goldman S, David P, et al. Stereotactic brain biopsy guided by positron emission tomography (PET) with [F-18]fluorodeoxyglucose and [C-11] methionine. *Acta Neurochir Suppl* 1997; 68:133–138
11. Pirotte B, Goldman S, Massager N, et al. Comparison of ^{18}F-FDG and ^{11}C-methionine for PET-guided stereotactic brain biopsy of gliomas. *J Nucl Med* 2004; 45:1293–1298
12. Pirotte BJ, Lubansu A, Massager N, Wikler D, Goldman S, Levivier M. Results of positron emission tomography guidance and reassessment of the utility of and indications for stereotactic biopsy in children with infiltrative brainstem tumors. *J Neurosurg* 2007; 107:392–399
13. Kawai N, Miyake K, Nishiyama Y, et al. Targeting optimal biopsy location in basal ganglia germinoma using (11)C-methionine positron emission tomography. *Surg Neurol* 2008; 70:408–413; discussion, 413
14. Goldman S, Levivier M, Pirotte B, et al. Regional methionine and glucose uptake in high-grade gliomas: a comparative study on PET-guided stereotactic biopsy. *J Nucl Med* 1997; 38:1459–1462
15. Go KG, Keuter EJ, Kamman RL, et al. Contribution of magnetic resonance spectroscopic imaging and L-[1-^{11}C]tyrosine positron emission tomography to localization of cerebral gliomas for biopsy. *Neurosurgery* 1994; 34:994–1002; discussion, 1002
16. Hara T, Kondo T, Hara T, Kosaka N. Use of ^{18}F-choline and ^{11}C-choline as contrast agents in positron emission tomography imaging-guided stereotactic biopsy sampling of gliomas. *J Neurosurg* 2003; 99:474–479
17. Misch M, Guggemos A, Driever PH, et al. (18)F-FET-PET guided surgical biopsy and resection in children and adolescence with brain tumors. *Childs Nerv Syst* 2015; 31:261–267
18. Lopez WO, Cordeiro JG, Albicker U, et al. Correlation of (18)F-fluoroethyl tyrosine positron-emission tomography uptake values and histomorphological findings by stereotactic serial biopsy in newly diagnosed brain tumors using a refined software tool. *Onco Targets Ther* 2015; 8:3803–3815
19. Kondo A, Ishii H, Aoki S, et al. Phase IIa clinical study of [^{18}F]fluciclovine: efficacy and safety of a new PET tracer for brain tumors. *Ann Nucl Med* 2016; 30:608–618
20. Pafundi DH, Laack NN, Youland RS, et al. Biopsy validation of ^{18}F-DOPA PET and biodistribution in gliomas for neurosurgical planning and radiotherapy target delineation: results of a prospective pilot study. *Neuro Oncol* 2013; 15:1058–1067
21. Price SJ, Fryer TD, Cleij MC, et al. Imaging regional variation of cellular proliferation in gliomas using 3′-deoxy-3′-[^{18}F]fluorothymidine positron-emission tomography: an image-guided biopsy study. *Clin Radiol* 2009; 64:52–63
22. Masada T, Takayama K, Kunishio K, Nagao S. Stereotactically inserted tube-guided brain biopsy using positron emission tomography and magnetic resonance coregistered images: case report. *Neurol Med Chir (Tokyo)* 2004; 44:209–212
23. Guo X, Guo Y, Cheng X, et al. Application of positron-emission tomography-magnetic resonance imaging fusion in biopsy and resection of gliomas. *Zhonghua Yi Xue Za Zhi* 2013; 93:15–18
24. Grech-Sollars M, Vaqas B, Thompson G, et al. An MRS- and PET-guided biopsy tool for intraoperative neuronavigational systems. *J Neurosurg* 2016; 11:1–7
25. Pezeshk P, Sadow CA, Winalski CS, Lang PK, Ready JE, Carrino JA. Usefulness of ^{18}F-FDG PET-directed skeletal biopsy for metastatic neoplasm. *Acad Radiol* 2006; 13:1011–1015
26. Werner MK, Aschoff P, Reimold M, Pfannenberg C. FDG-PET/CT-guided biopsy of bone metastases sets a new course in patient management after extensive imaging and multiple futile biopsies. *Br J Radiol* 2011; 84:e65–e67
27. Nanni C, Gasbarrini A, Cappelli A, et al. FDG PET/CT for bone and soft-tissue biopsy. *Eur J Nucl Med Mol Imaging* 2015; 42:1333–1334
28. Purandare NC, Kulkarni AV, Kulkarni SS, et al. ^{18}F-FDG PET/CT-directed biopsy: does it offer incremental benefit? *Nucl Med Commun* 2013; 34:203–210
29. Maybody M, Grewal RK, Healey JH, et al. Ga-68 DOTATOC PET/CT-guided biopsy and cryoablation with autoradiography of biopsy specimen for treatment of tumor-induced osteomalacia. *Cardiovasc Intervent Radiol* 2016; 39:1352–1357
30. Guo W, Hao B, Chen HJ, et al. PET/CT-guided percutaneous biopsy of FDG-avid metastatic bone lesions in patients with advanced lung cancer: a safe and effective technique. *Eur J Nucl Med Mol Imaging* 2017; 44:25–32
31. Kim J, Lee J, Chang E, et al. Selective sentinel node plus additional non-sentinel node biopsy based on an FDG-PET/CT scan in early breast cancer patients: single institutional experience. *World J Surg* 2009; 33:943–949
32. Challa VR, Srivastava A, Dhar A, et al. Role of fluorine-18-labeled 2-fluoro-2-deoxy-D-glucose positron emission tomography-computed tomography in the evaluation of axillary lymph node involvement in operable breast cancer in comparison with sentinel lymph node biopsy. *Indian J Nucl Med* 2013; 28:138–143
33. Siepel FJ, de Bruin WI, van Duyn EB, et al. Targeted lymph node biopsy in mediastinoscopy using 3D FDG-PET/CT movies: a feasibility study. *Nucl Med Commun* 2012; 33:439–444
34. Györke T, Kollár A, Bottlik G,, et al. Radioguided lymph node biopsy of a chemoresistant lymph node detected on interim FDG PET-CT in Hodgkin lymphoma. *Int J Hematol* 2011; 93:545–550
35. Juweid ME, Smith B, Itti E, Meignan M. Can the interim fluorodeoxyglucose-positron emission to-

mography standardized uptake value be used to determine the need for residual mass biopsy after dose-dense immunochemotherapy for advanced diffuse large B-cell lymphoma? *J Clin Oncol* 2010; 28:e719–e720

36. Kalinyak JE, Schilling K, Berg WA, et al. PET-guided breast biopsy. *Breast J* 2011; 17:143–151
37. Raylman RR, Majewski S, Smith MF, et al. The positron emission mammography/tomography breast imaging and biopsy system (PEM/PET): design, construction and phantom-based measurements. *Phys Med Biol* 2008; 53:637–653
38. Islam S, Walker RC. Advanced imaging (positron emission tomography and magnetic resonance imaging) and image-guided biopsy in initial staging and monitoring of therapy of lung cancer. *Cancer J* 2013; 19:208–216
39. Beggs AD, Hain SF, Curran KM, O'Doherty MJ. FDG-PET as a "metabolic biopsy" tool in non-lung lesions with indeterminate biopsy. *Eur J Nucl Med Mol Imaging* 2002; 29:542–546
40. Niida T, Isoda K, Miyazaki K, et al. Pulmonary intravascular lymphoma diagnosed by 18-fluorodeoxyglucose positron emission tomography-guided transbronchial lung biopsy in a man with long-term survival: a case report. *J Med Case Rep* 2011; 5:295
41. Collins BT, Lowe VJ, Dunphy FR. Initial evaluation of pulmonary abnormalities: CT-guided fine-needle aspiration biopsy and fluoride-18 fluorodeoxyglucose positron emission tomography correlation. *Diagn Cytopathol* 2000; 22:92–96
42. İntepe YS, Metin B, Şahin S, Kaya B, Okur A. Our transthoracic biopsy practices accompanied by the imaging process: the contribution of positron emission tomography usage to accurate diagnosis. *Acta Clin Belg* 2016; 71:214–220
43. Lin E. FDG PET/CT for biopsy guidance in Erdheim-Chester disease. *Clin Nucl Med* 2007; 32:860–861
44. Yokoyama K, Ikeda O, Kawanaka K, et al. Comparison of CT-guided percutaneous biopsy with and without registration of prior PET/CT images to diagnose mediastinal tumors. *Cardiovasc Intervent Radiol* 2014; 37:1306–1311
45. Luketich JD, Schauer P, Urso K, et al. Minimally invasive surgical biopsy confirms PET findings in esophageal cancer. *Surg Endosc* 1997; 11:1213–1215
46. Mizugaki H, Shinagawa N, Kanegae K, et al. Combining transbronchial biopsy using endobronchial ultrasonography with a guide sheath and positron emission tomography for the diagnosis of small peripheral pulmonary lesions. *Lung Cancer* 2010; 68:211–215
47. von Rahden BH, Sarbia M, Stein HJ. Medical image: combined FDG-PET/CT and CT-guided biopsy in diagnosing oesophageal cancer recurrence. *N Z Med J* 2006; 119:U1810
48. Collins BT, Gardner LJ, Verma AK, Lowe VJ, Dunphy FR, Boyd JH. Correlation of fine needle aspiration biopsy and fluoride-18 fluorodeoxyglucose positron emission tomography in the assessment of locally recurrent and metastatic head and neck neoplasia. *Acta Cytol* 1998; 42:1325–1329
49. Kovács AF, Döbert N, Gaa J, Menzel C, Bitter K. Positron emission tomography in combination with sentinel node biopsy reduces the rate of elective neck dissections in the treatment of oral and oropharyngeal cancer. *J Clin Oncol* 2004; 22:3973–3980
50. Reinbacher KE, Pau M, Wallner J, et al. Minimal invasive biopsy of intraconal expansion by PET/CT/MRI image-guided navigation: a new method. *J Craniomaxillofac Surg* 2014; 42:1184–1189
51. Tatli S, Gerbaudo VH, Feeley CM, Shyn PB, Tuncali K, Silverman SG. PET/CT-guided percutaneous biopsy of abdominal masses: initial experience. *J Vasc Interv Radiol* 2011; 22:507–514
52. Tatli S, Gerbaudo VH, Mamede M, Tuncali K, Shyn PB, Silverman SG. Abdominal masses sampled at PET/CT-guided percutaneous biopsy: initial experience with registration of prior PET/CT images. *Radiology* 2010; 256:305–311
53. Aparici CM, Win AZ. Use of positron emission tomography/CT to perform biopsy of a mesenteric mass. *J Vasc Interv Radiol* 2014; 25:1609
54. Shao H, Cheng W, Yu L, Li Y, Jing H. Use of ^{18}F-FDG PET scan and ultrasound-guided biopsy in the diagnosis of hepatic carcinomas. *Hepatogastroenterology* 2015; 62:978–981
55. Collins BT, Lowe VJ, Dunphy FR. Correlation of CT-guided fine-needle aspiration biopsy of the liver with fluoride-18 fluorodeoxyglucose positron emission tomography in the assessment of metastatic hepatic abnormalities. *Diagn Cytopathol* 1999; 21:39–42
56. Yu HY, Sheng JF. Liver tuberculosis presenting as an uncommon cause of pyrexia of unknown origin: positron emission tomography/computed tomography identifies the correct site for biopsy. *Med Princ Pract* 2014; 23:577–579
57. Ewertsen C, Henriksen BM, Torp-Pedersen S, Bachmann Nielsen M. Characterization by biopsy or CEUS of liver lesions guided by image fusion between ultrasonography and CT, PET/CT or MRI. *Ultraschall Med* 2011; 32:191–197
58. Imperiale A, Garnon J, Bachellier P, Gangi A, Namer IJ. Simultaneous (18)F-FDOPA PET/CT-guided biopsy and radiofrequency ablation of recurrent neuroendocrine hepatic metastasis: further step toward a theranostic approach. *Clin Nucl Med* 2015; 40:e334–e335
59. Schuster DM, Votaw JR, Nieh PT, et al. Initial experience with the radiotracer anti-1-amino-3-F-18-fluorocyclobutane-1-carboxylic acid with PET/CT in prostate carcinoma. *J Nucl Med* 2007; 48:56–63
60. Schuster DM, Taleghani PA, Nieh PT, et al. Characterization of primary prostate carcinoma by anti-1-amino-2-[^{18}F]-fluorocyclobutane-1-carboxylic acid (anti-3-[^{18}F] FACBC) uptake. *Am J Nucl Med Mol Imaging* 2013; 3:85–96
61. Fei B, Nieh PT, Schuster DM, Master VA. PET-directed, 3D ultrasound-guided prostate biopsy. *Diagn Imaging Eur* 2013; 29:12–15
62. Fei B, Schuster DM, Master V, Akbari H, Fenster A, Nieh P. A molecular image–directed, 3D ultrasound-guided biopsy system for the prostate. *Proc SPIE Int Soc Opt Eng* 2012; 2012:831613
63. Fei B, Master V, Nieh P, et al. A PET/CT directed, 3D ultrasound-guided biopsy system for prostate cancer. *Prostate Cancer Imaging* 2011; 6363:100–108
64. Fei B, Nieh PT, Master VA, Zhang Y, Osunkoya AO, Schuster DM. Molecular imaging and fusion targeted biopsy of the prostate. *Clin Transl Imaging* 2017; 5:29–43
65. Freesmeyer M, Drescher R, Winkens T. Unexpected diagnosis of peripheral schwannoma on ^{18}F-fluoroethylcholine PET/CT for localization of prostate cancer recurrence and biopsy under real-time PET/ultrasound fusion guidance. *Clin Nucl Med* 2014; 39:385–386
66. Garcia-Bennett J, Henriquez I, Zugazaga Cortazar A, Fuertes J. Needle track recurrence after transrectal prostate biopsy detected by (1)(8)F-choline PET-CT. *Rev Esp Med Nucl Imagen Mol* 2015; 34:128–129
67. Kwee SA, DeGrado T. Prostate biopsy guided by ^{18}F-fluorocholine PET in men with persistently elevated PSA levels. *Eur J Nucl Med Mol Imaging* 2008; 35:1567–1569
68. Igerc I, Kohlfurst S, Gallowitsch HJ, et al. The value of ^{18}F-choline PET/CT in patients with elevated PSA-level and negative prostate needle biopsy for localisation of prostate cancer. *Eur J Nucl Med Mol Imaging* 2008; 35:976–983
69. Takei T, Souvatzoglou M, Beer AJ, et al. A case of multimodality multiparametric ^{11}C-choline PET/MR for biopsy targeting in prior biopsy-negative primary prostate cancer. *Clin Nucl Med* 2012; 37:918–919
70. Jadvar H, Chen K, Ukimura O. Targeted prostate gland biopsy with combined transrectal ultrasound, mpMRI, and ^{18}F-FMAU PET/CT. *Clin Nucl Med* 2015; 40:e426–e428
71. Mallarajapatna GJ, Kallur KG, Ramanna NK, Susheela SP, Ramachandra PG. PET/CT-guided percutaneous biopsy of isolated intramuscular metastases from postcricoid cancer. *J Nucl Med Technol* 2009; 37:220–222
72. O'Sullivan PJ, Rohren EM, Madewell JE. Positron emission tomography-CT imaging in guiding musculoskeletal biopsy. *Radiol Clin North Am* 2008; 46:475–486
73. Hain SF, O'Doherty MJ, BinghAm J, Chinyama C, Smith MA. Can FDG PET be used to successfully direct preoperative biopsy of soft tissue tumours? *Nucl Med Commun* 2003; 24:1139–1143
74. Fanchon L, Carlin S, Burger I, et al. MO-G-17A-09: quantitative autoradiography of biopsy specimens extracted under PET/CT guidance. *Med Phys* 2014; 41:439
75. Fanchon LM, Dogan S, Moreira AL, et al. Feasibility of in situ, high-resolution correlation of tracer uptake with histopathology by quantitative autoradiography of biopsy specimens obtained under ^{18}F-FDG PET/CT guidance. *J Nucl Med* 2015; 56:538–544

(Figures start on next page)

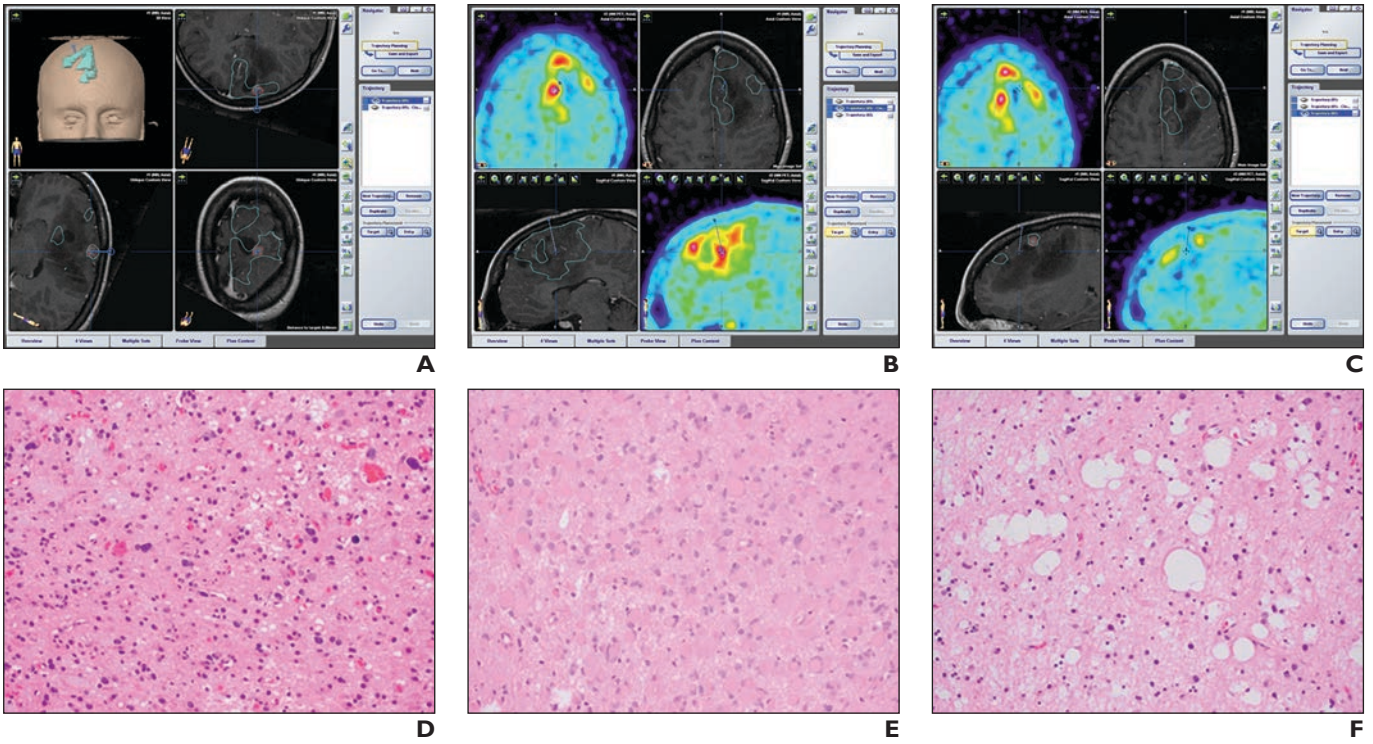

Fig. 1—19-year-old woman with Li-Fraumeni syndrome and astrocytoma (World Health Organization grade 2) and regional variability of histologic characteristics. (Reprinted with permission from [17])
A–C, Screen shots from intraoperative neuronavigation show different ROIs with PET positivity and MRI contrast enhancement (**A**), PET positivity without contrast enhancement (**B**), and PET negativity without contrast enhancement (**C**).
D–F, Photomicrographs of tumor samples corresponding to **A–C** show solid tumor (pleomorphic glial tumor cells) (**D**), infiltration zone (gemistocytic glial tumor cells) (**E**), and solid tumor (cystic glial fibrillary matrix) (**F**).

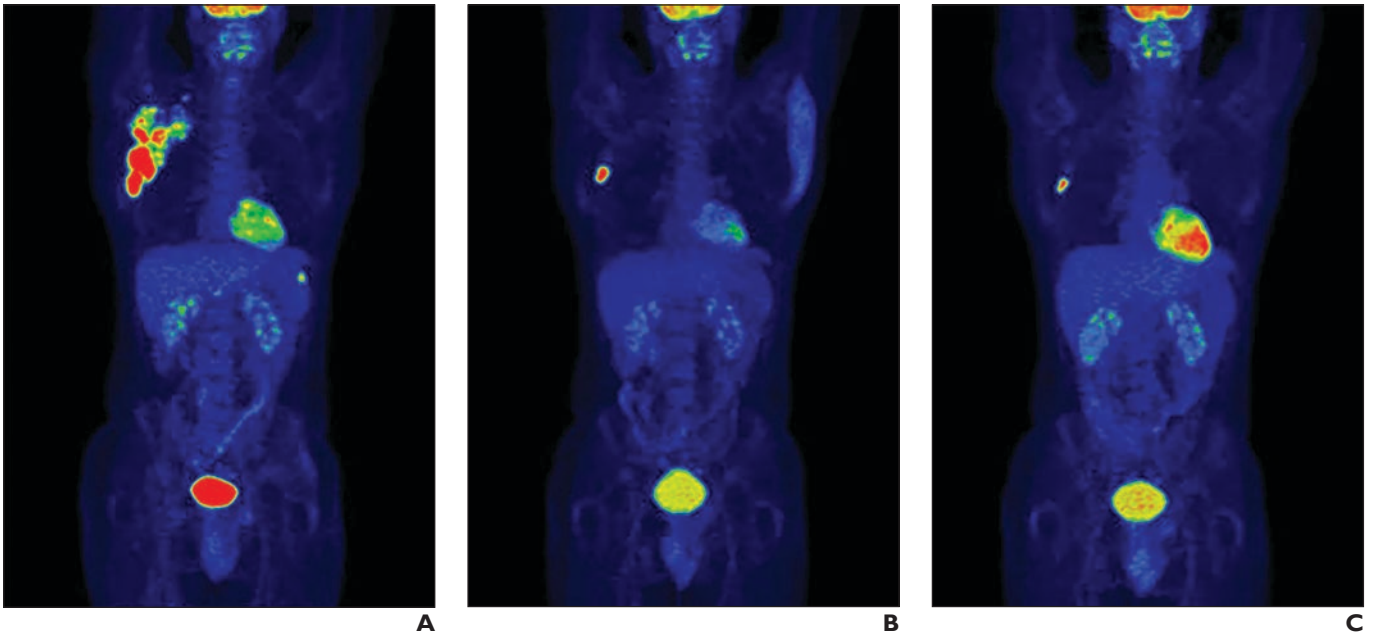

Fig. 2—32-year-old man with painless right axillary lymph node enlargement.
A–I, Staging (**A, D, G**), interim (**B, E, H**), and second interim (**C, F, I**) maximum-intensity-projection PET images (**A–C**) and transverse fused PET/CT slices in two levels of axilla (**D–F, G–I**). Staging PET/CT image (**A**) shows widespread right axillary involvement and focal uptake in spleen. Interim images show good metabolic response both in axilla and in spleen, except one single enlarged axillary lymph node (**E**). Several similarly enlarged but metabolically inactive further lymph nodes are present in right axilla (**G–I**). (Reprinted with permission from [34])

(Fig. 2 continues on next page)

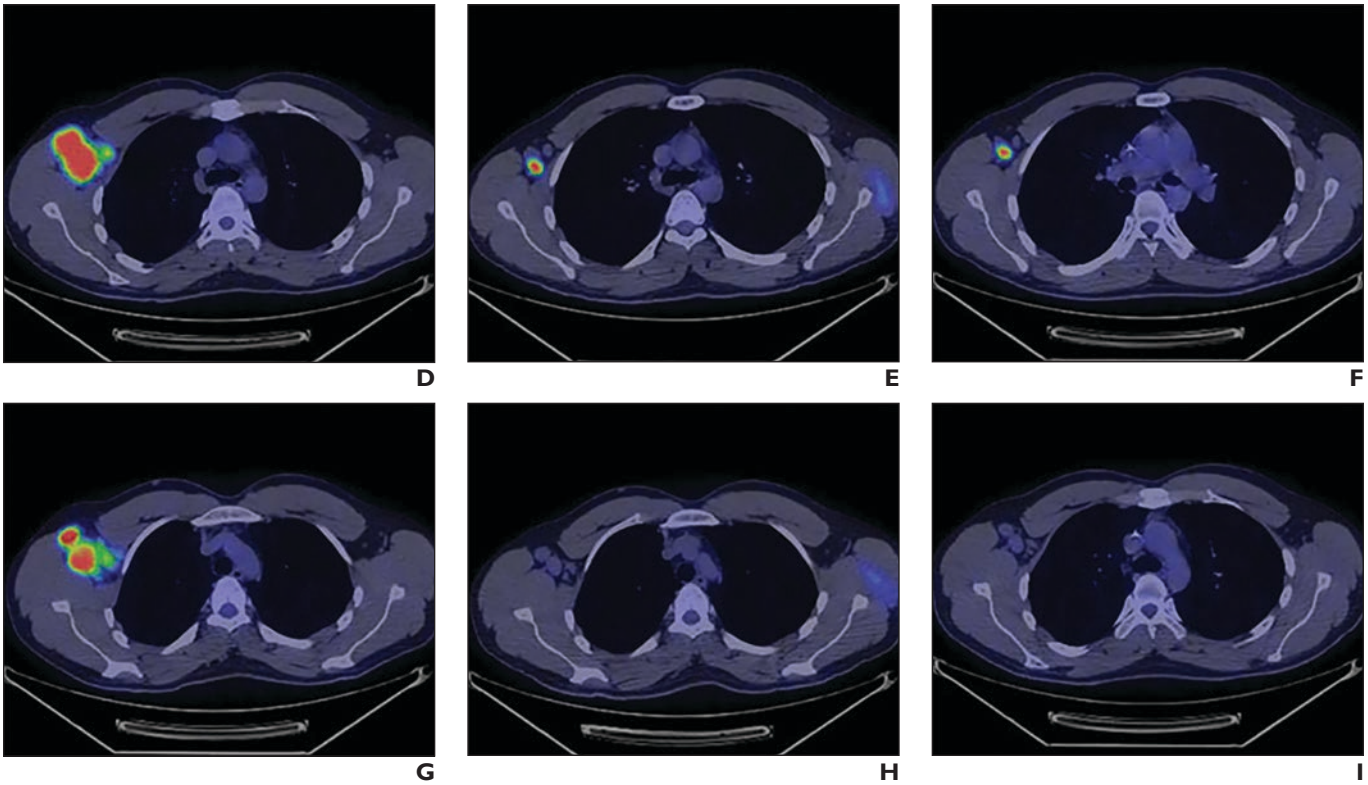

Fig. 2 (continued)—32-year-old man with painless right axillary lymph node enlargement.
A–I, Staging (**A, D, G**), interim (**B, E, H**), and second interim (**C, F, I**) maximum-intensity-projection PET images (**A–C**) and transverse fused PET/CT slices in two levels of axilla (**D–F, G–I**). Staging PET/CT image (**A**) shows widespread right axillary involvement and focal uptake in spleen. Interim images show good metabolic response both in axilla and in spleen, except one single enlarged axillary lymph node (**E**). Several similarly enlarged but metabolically inactive further lymph nodes are present in right axilla (**G–I**). (Reprinted with permission from [34])

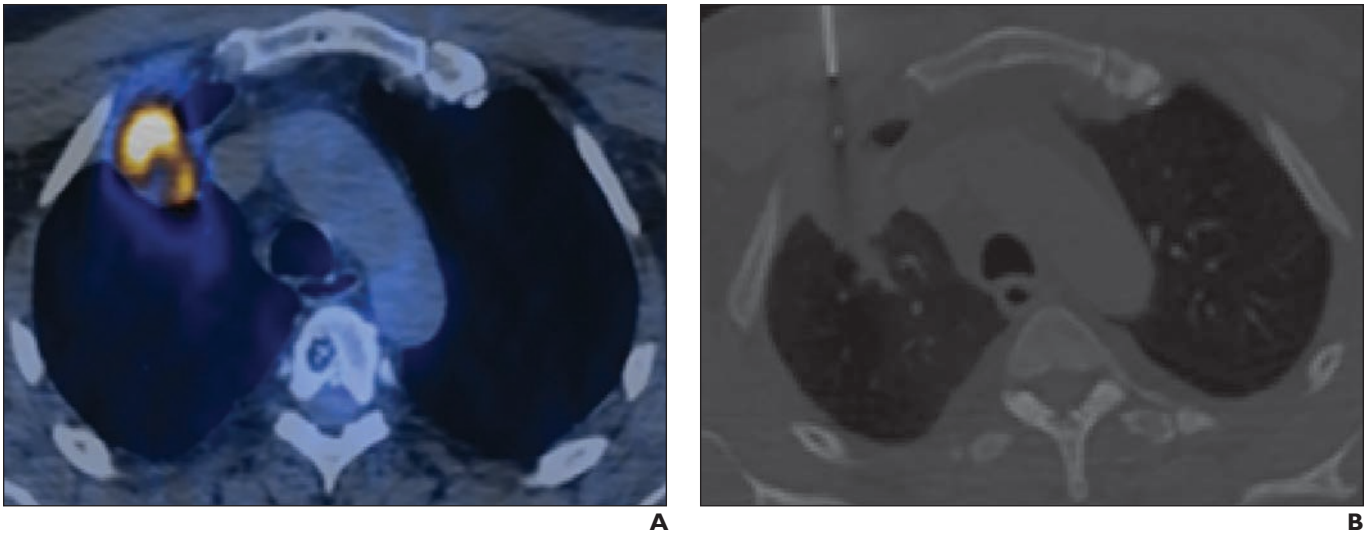

Fig. 3—PET (**A**) and CT (**B**) images show area targeted for biopsy. (Reprinted with permission from [42])

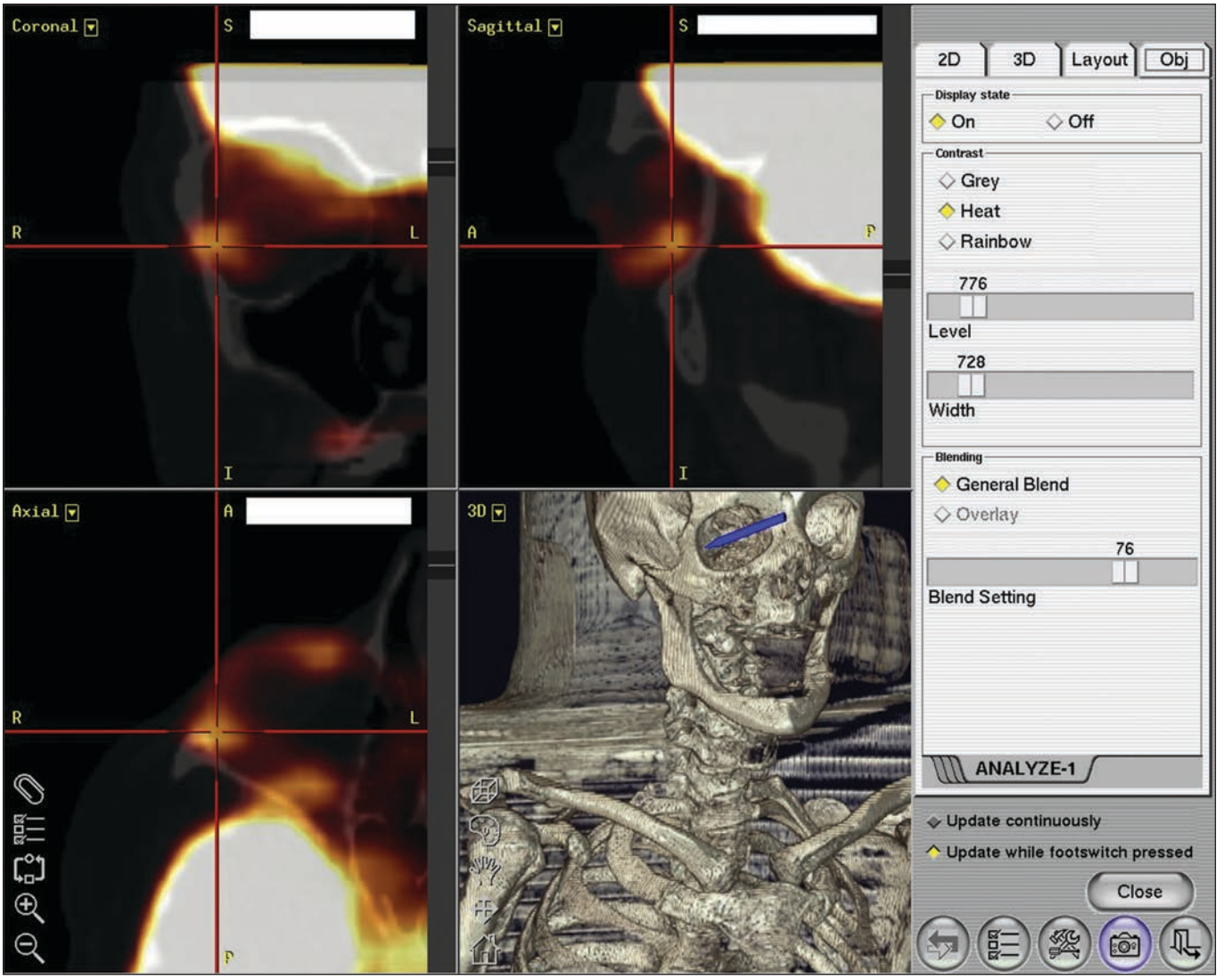

Fig. 4—Screen shot shows preoperative planning at workstation. Crosshairs indicate lesion to be biopsied. Arrow indicates location of lesion in bony orbit. (Reprinted with permission from [50])

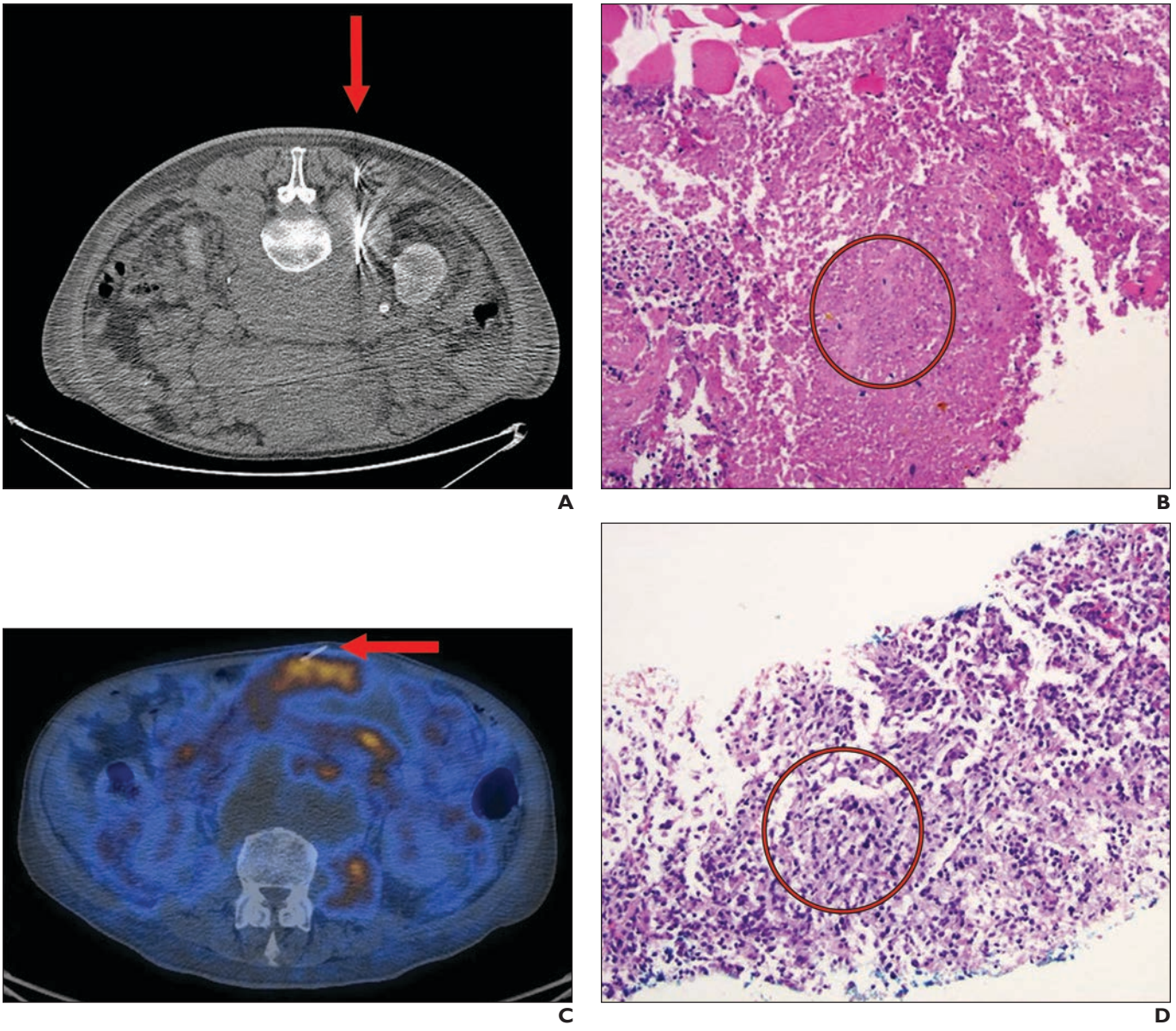

Fig. 5—61-year-old man with follicular lymphoma and mixed response to chemotherapy. (Reprinted with permission from [53])
A, CT image obtained during biopsy (*arrow*) of retroperitoneal mass shows predominantly necrotic tissue.
B, Photomicrograph shows necrotic tissue (*circle*) from lesion in **A**. Viable muscle is present only at upper left.
C, Follow-up PET/CT showed new mesenteric mass suspicious for malignancy. Real-time intraprocedural image obtained during PET-guided biopsy (*arrow*) shows new mesenteric mass.
D, Photomicrograph of lesion in **C** shows Bcl-2–positive poorly defined lymphoid follicles (*circle*) compatible with follicular lymphoma.

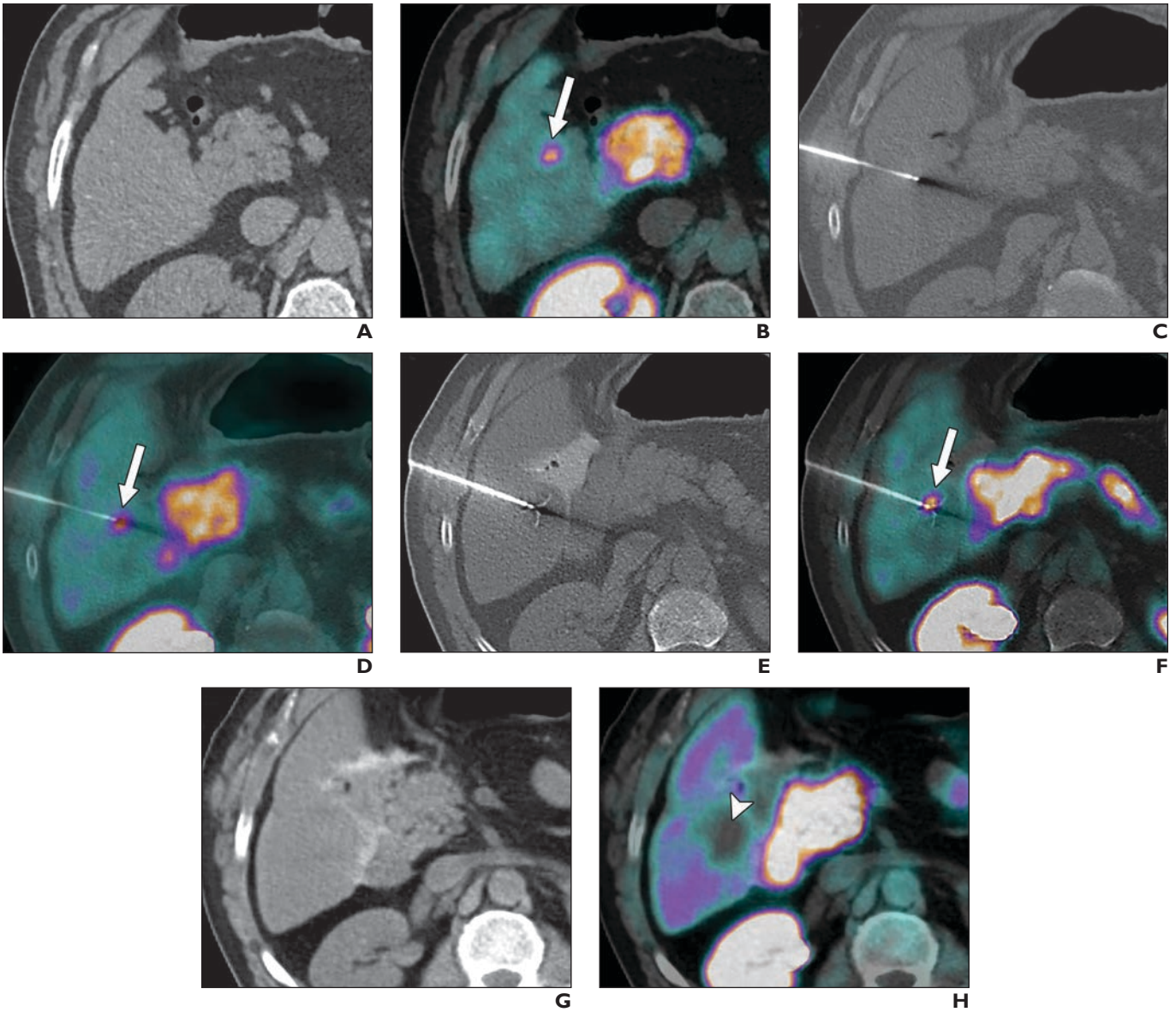

Fig. 6—57-year-old man with history of well-differentiated ileal neuroendocrine tumor and progressive increase in chromogranin A and 5-hydroxyindoleacetic acid levels referred for further evaluation. Conventional radiologic investigations revealed no clinically significant abnormalities. However, ^{18}F-fluorodihydroxyphenylalanine (FDOPA) PET/CT showed focal pathologic radiotracer uptake in segment V of liver, suggesting relapsing disease. As recommended by local multidisciplinary board, PET/CT-guided biopsy and liver radiofrequency ablation (RFA) were scheduled. PET/CT was performed under general anesthesia without IV contrast enhancement. (Reprinted with permission from [58])

A and **B,** Single-bed-position PET/CT acquisition including target lesion was performed 30 minutes after IV injection of 259 MBq FDOPA. PET, CT (**A**), and PET/CT (**B**) images were reviewed side-by-side, and 14-gauge coaxial needle was introduced stepwise under CT guidance. Arrow indicates radiotracer uptake.

C and **D,** CT (**C**), and PET/CT (**D**) images show correct position of needle in hypermetabolic lesion before performance of diagnostic biopsy. Arrow indicates radiotracer uptake.

E and **F,** CT (**E**) and PET/CT (**F**) images show coaxial insertion of 18-gauge core biopsy needle. Two samples were obtained for histologic analysis. Afterward, expandable 15-gauge, 4-cm-diameter RF probe was deployed through coaxial needle and placed in same biopsy location. Proper positioning of all tines of RF probe was assured with single-bed-position PET/CT. Thus, RF current was increased slowly according to dedicated protocol for liver with maximum power of 180 W. Second RF application was performed after 1.5-cm withdrawal of RF probe. Total duration of RFA was 30 minutes. Arrow indicates radiotracer uptake.

G and **H,** CT (**G**) and PET/CT (**H**) images obtained approximately 30 minutes after end of RFA show photopenia at ablated site (*arrowhead*). No early or late complications were described. Metastatic origin of neuroendocrine tumor was established at pathologic examination.

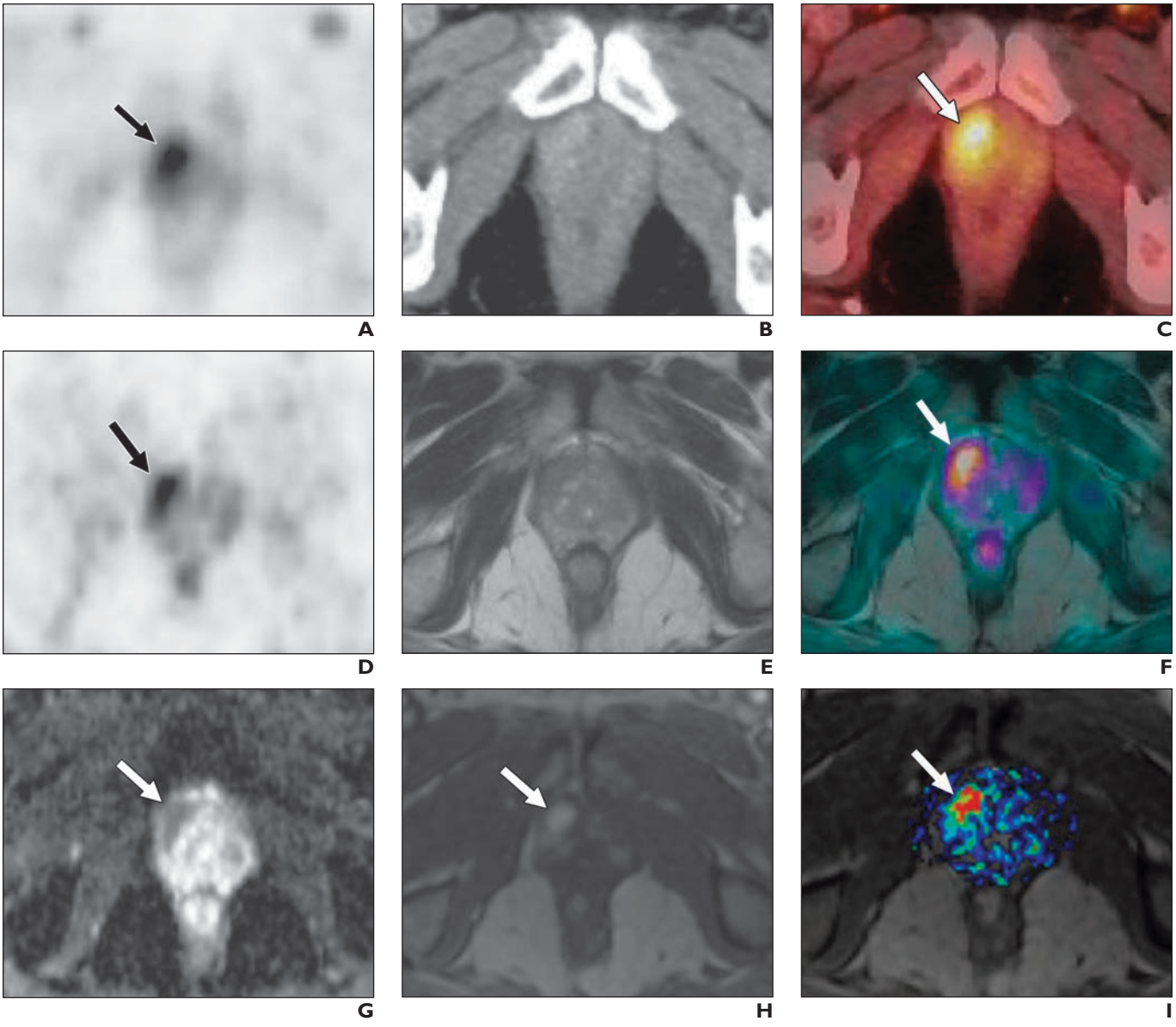

Fig. 7—70-year-old man with elevated prostate-specific antigen level (17.7 ng/mL) and previous negative transrectal biopsy result. Carbon-11-labeled choline PET/CT was performed 5 minutes after IV injection of 812 MBq (21.95 mCi) of ^{11}C-labeled choline (3 minutes per bed position) combined with diagnostic portal venous phase CT. (Reprinted with permission from [69])

A, Choline PET image shows intense focal uptake behind symphysis on right (*arrow*).

B, CT image shows only slight and unspecific contrast enhancement in region shown in **A.**

C, Fusion PET/CT image confirms ventral location of focal choline uptake (*arrow*) in right apex of prostate gland.

D and **E,** After completion of PET/CT, patient underwent PET/MRI starting 30 minutes after tracer injection (4 minutes per bed position). In region with high focal uptake at PET (*arrow*, **D**), T2-weighted MR image (**E**) shows hypointense area in ventral peripheral zone suspicious for prostate cancer.

F, Fused PET/MRI dataset shows anatomic concordance (*arrow*) between PET and T2-weighted MRI findings.

G–I, Additional evidence of prostate cancer in area in **A–F** was visualized with multiparametric functional MRI. DW image (**G**) shows highly restricted diffusion (*arrow*), and dynamic contrast-enhanced MR image shows intense focal enhancement (*arrow*) in early phase (**H**) with high value of AUC within 60 seconds (**I**), indicating rapid wash-in of contrast medium (*arrow*). Rebiopsy based on these findings had positive result, guiding patient toward appropriate treatment, that is, radical prostatectomy.

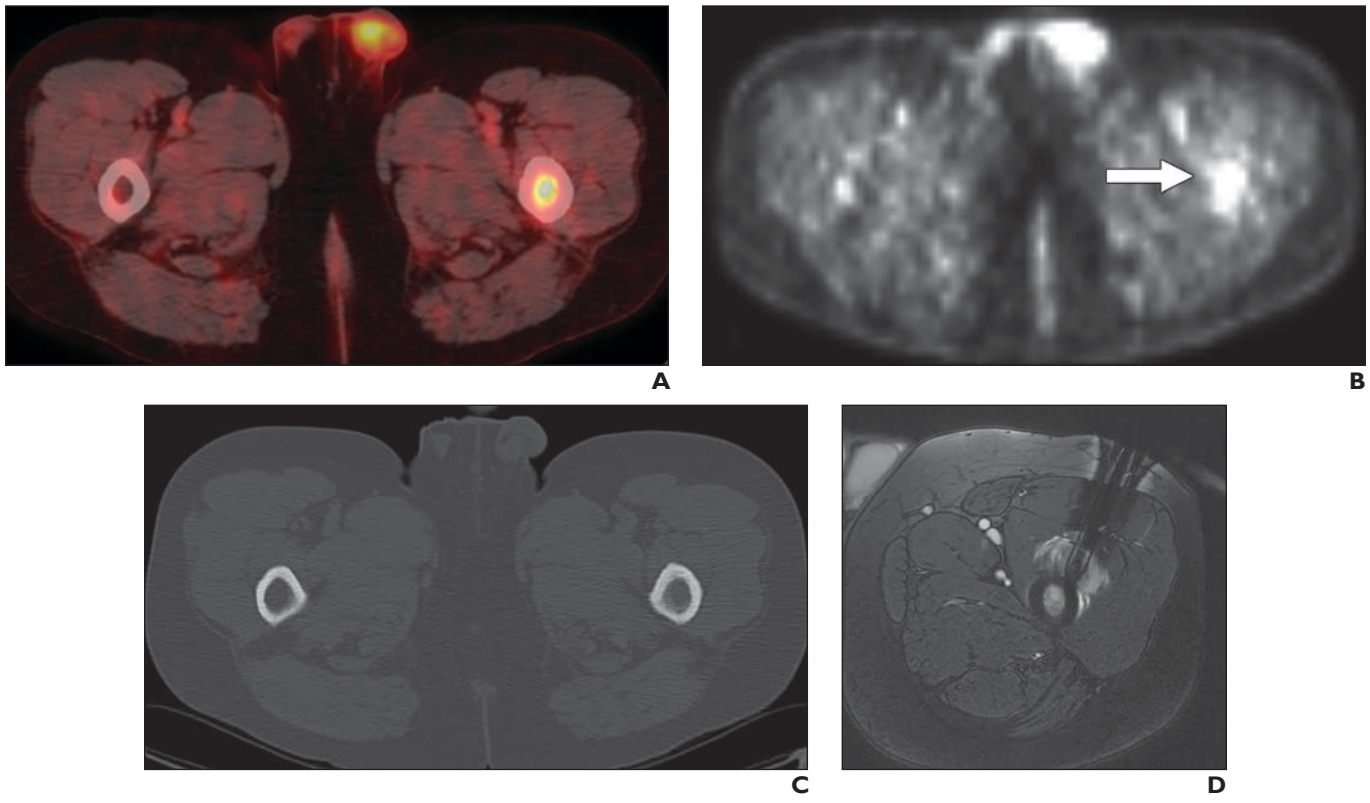

Fig. 8—48-year-old man with mucinous adenocarcinoma of anus. (Reprinted with permission from [72])
A, Fused PET/CT image of pelvis shows hypermetabolic metastases in left femur. Normal increased FDG activity is evident in left testis.
B, Unfused PET image shows focus of increased activity (*arrow*) in left femur.
C, CT image shows no definite abnormality in femur.
D, Image obtained during MRI-guided biopsy shows increased signal intensity in femoral metastases and signal-intensity void from contours of core biopsy needle.

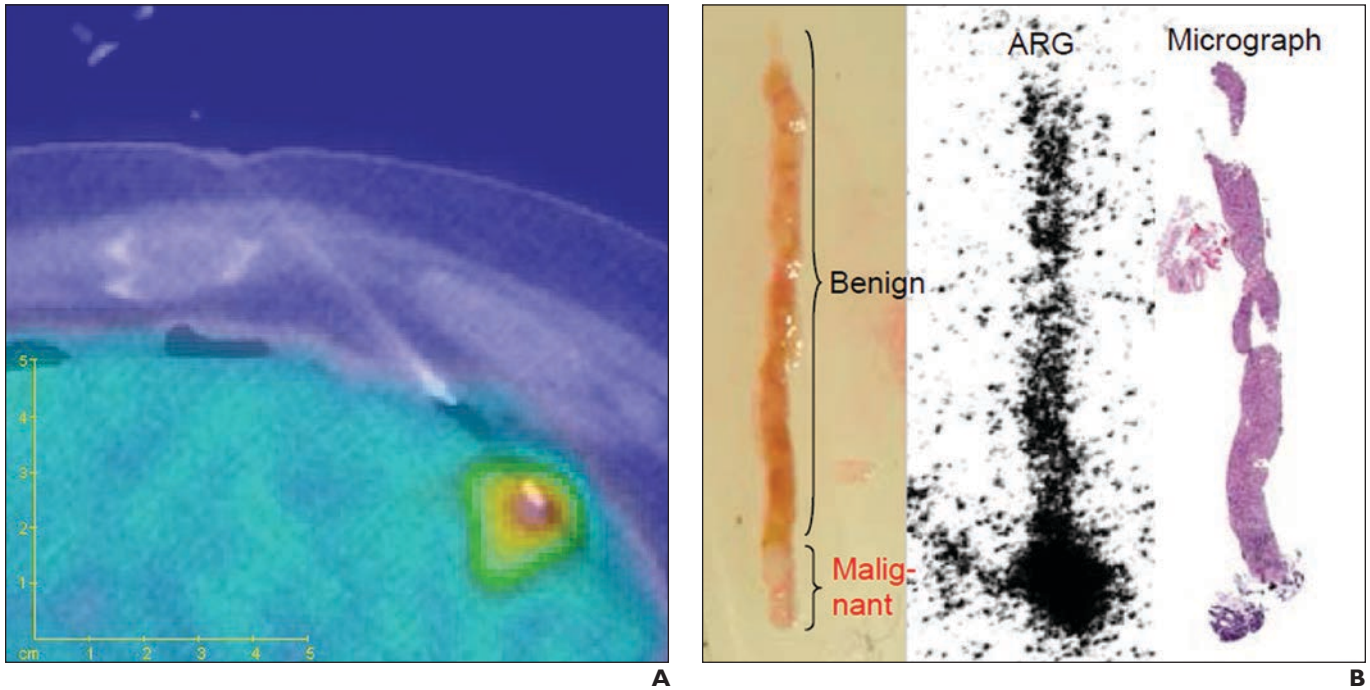

Fig. 9—Correlation of PET and biopsy specimens. (Reprinted with permission from [75])
A, Fused PET/CT image shows peripheral needle placement with both malignant and benign tissue.
B, Extracted photograph, autoradiograph (ARG), and micrograph show specimen.

(Fig. 9 continues on next page)

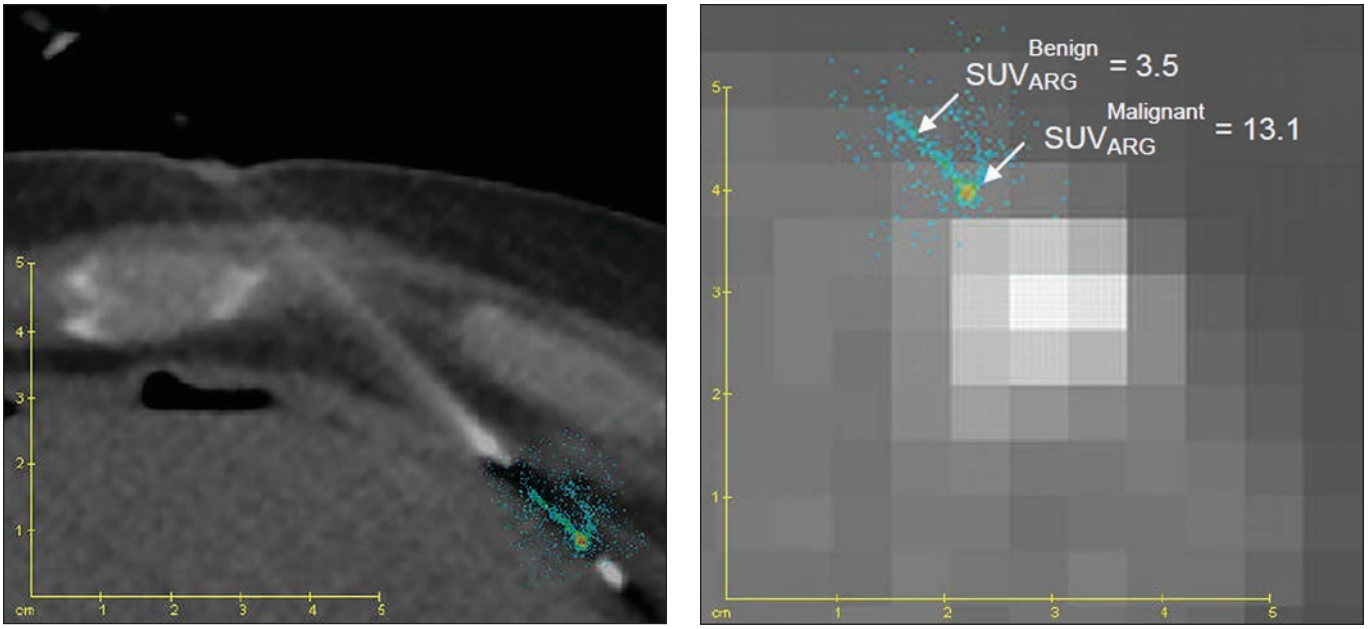

Fig. 9 (continued)—Correlation of PET and biopsy specimens. (Reprinted with permission from [75])
C and **D,** Fusion of ARG with CT (**C**) and PET (**D**) images. SUV = standardized uptake value.

FOR YOUR INFORMATION

This article is available for CME and Self-Assessment (SA-CME) credit that satisfies Part II requirements for maintenance of certification (MOC). To access the examination for this article, follow the prompts associated with the online version of the article.